

Real-Time Demonstration of 2.4Tbps (200Gbps/ λ) Bidirectional Coherent DWDM-PON Enabled by Coherent Nyquist Subcarriers

A. Rashidinejad¹, A. Nguyen², M. Olson³, S. Hand², and D. Welch²

¹: Infinera Canada, 555 Legget Drive, Suite 222, Ottawa, ON, Canada

²: Infinera Corporation, 140 Caspian Court., Sunnyvale, CA, USA

³: Infinera Sweden, Fredsborgsgatan 24, 117 43 Stockholm, Sweden

arashidinejad@infinera.com

Abstract: We demonstrate real-time 2.4Tbps bidirectional coherent DWDM-PON (12 λ ×200Gbps/ λ) over 100km SMF, enabled by multiplexing Nyquist subcarriers. Further, through proof-of-concept experiments, we show the advantage of coherent subcarrier aggregation in next-generation point-to-multipoint bidirectional access networks.

OCIS codes: (060.1660) Coherent Communications; (060.4252) Networks, Broadcast

1. Introduction

Optical access aggregation has been traditionally based on low-speed (<10Gbps) Intensity Modulation and Direct Detection (IMDD) formats, that despite their simplicity, suffer from low spectral efficiency, poor receiver sensitivity, and vulnerability to chromatic dispersion [1]. As a result, network backbone providers are beginning to turn to coherent solutions that enable higher receiver sensitivity, high-order advanced modulation, and Dense Wavelength Division Multiplexing (DWDM), to support the ever-increasing bandwidth demand of 5G mobile networks, fiber deep, and next generation Internet of Things (IoT) [2]. Furthermore, limited fiber availability at the network edge has prompted research and development of low-cost single-fiber bidirectional transport solutions in such networks [3,4].

In this work, we demonstrate real-time 2.4Tbps bidirectional coherent DWDM-PON over an unamplified 100km SMF link, utilizing 12 optical carriers spaced at 50GHz and each carrying 100Gbps in either direction. In order to realize this, the up- and downlink data are multiplexed over different non-overlapping Nyquist subcarriers (SC), hence providing immunity to performance degradations from network reflection and back-scattering. We further investigate the advantage of coherent subcarrier aggregation in a high-speed point-to-multipoint bidirectional setup, where two low-cost coherent leaf nodes communicate with a high-capacity aggregation hub over a 50km bidirectional link.

2. High-Speed Bidirectional Point-to-Point Communication

Figure 1(a) depicts our Point-to-Point (P2P) experimental setup, designed to emulate high-capacity bidirectional communication between two central office (CO) aggregation nodes separated by 100km. Each station consists of a 12-laser coherent transceiver, a transmit and receive EDFA, and a high-isolation circulator. The coherent transceivers are comprised of Infinera's 4th generation PIC and DSP/ASIC [5,6] and are all configured to operate with 4 Nyquist subcarriers at ~8GBaud/s, dual-polarization 16-QAM, which considering FEC overhead, results in 50Gbps per subcarrier for each optical carrier. In order to prevent spectral overlap in the bidirectional link, each CO only transmits 100Gbps data over two of the four available SCs per wave, upper two SCs in uplink (blue) and lower two in downlink (red), as shown in the cartoon depictions of Figs. 1(b)-(c). By doing this, any reflections from network components, as well as back-scattering from the long fiber propagation, would be out of band at the corresponding coherent receivers and can thus be mitigated by digital filtering in the DSP. Finally, the 12 optical carriers in this experiment are spaced at 50GHz in the center of C-band, about ~193.8THz.

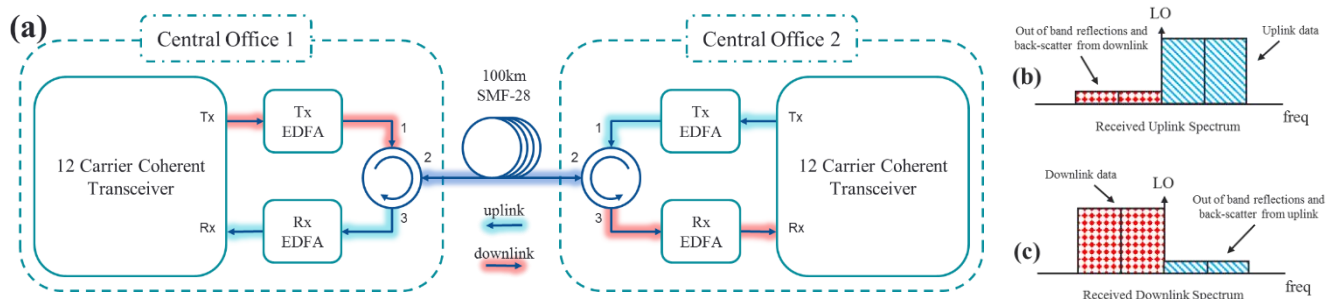


Fig. 1. (a) High-speed P2P bidirectional experimental setup; and cartoon depiction of (b) uplink and (c) downlink optical spectra for each carrier.

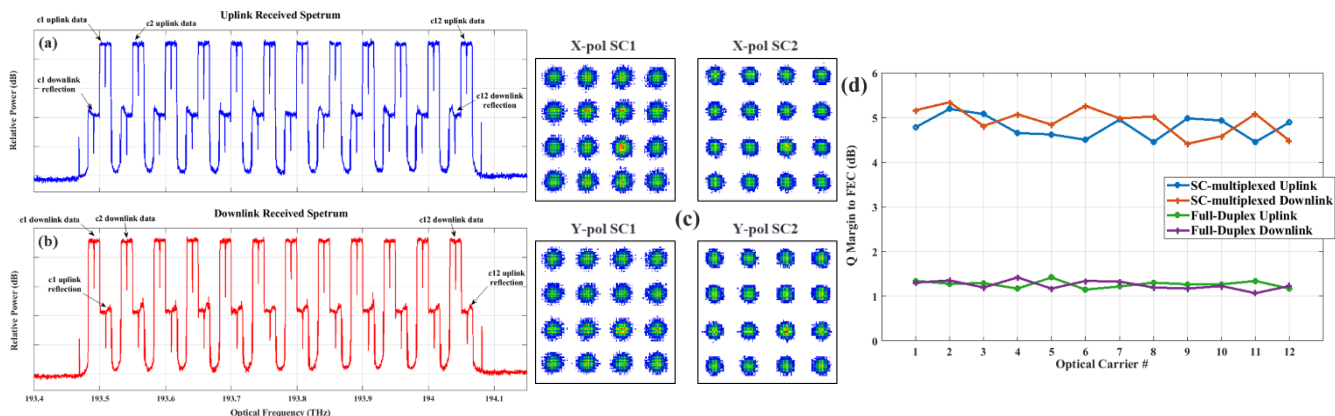


Fig. 2. Measurement results: Optical spectrum at receiver for (a) CO-1 (uplink) and (b) CO-2 (downlink); (c) Constellation diagrams for carrier 2 in the downlink direction measured at CO-2 Rx; (d) Q margin comparison of SC-multiplexed and full-duplex bidirectional communication.

Figures 2(a)-(b) show the measured optical spectra at each central office receiver. The 12 carriers can be observed in both captures, where 2 subcarriers hold more power than the other 2, which are due to reflection and back-scattering in the reverse direction. Due to the significant propagation distance (100km), the signal to reflection power ratio is relatively low as compared to background noise level. However, as described, the receiver on either station is programmed to filter out and remove the out-of-band reflection spectra and is thus not expected to be impacted by them. Figures 2(c) illustrates the constellation diagrams for carrier 2 in the downlink direction (polarizations X and Y, and SCs 1 and 2) as a representative example of the observed performance in this demonstration. As can be inferred from these constellations, error-free real-time coherent communication is successfully accomplished with a very good margin to FEC limit for all 12 channels in both transmission directions, adding up to a record 2.4Tbps bidirectionally over the 100km fiber (1.2Tbps in each direction).

Next, we compare the Q margin to FEC threshold for the aforementioned subcarrier-multiplexed configuration and the case where both CO-1 and CO-2 transmit data over all 4 SCs, i.e. full-duplex. The results of this comparison, accumulated for 1 hour, are plotted in Fig. 2(d). Even though utilizing all 4 SCs in both uplink and downlink provides two times spectral efficiency, but this is achieved at the cost of susceptibility to reflections and back-scattering. In the setup of Fig. 1(a), after 100km bidirectional propagation, an average Q penalty of 3.59dB is observed between the two configurations. Moreover, as the signal to reflection ratio decreases (with an increase in bidirectional propagation distance), the full-duplex configuration suffers more and more from OSNR reduction and accumulates an even higher Q penalty to the point where a much stronger FEC would be needed to maintain error-free communication.

3. Subcarrier-Multiplexed Bidirectional Point-to-Multipoint Coherent Access

To further demonstrate the advantage that Nyquist subcarriers provide in bidirectional coherent access networks, we conduct a proof-of-concept point-to-multipoint experiment on the setup of Fig. 3(a). In this configuration, a single-laser high-capacity aggregation hub broadcasts high-speed data to/from lower-speed remote nodes over a 50km SMF bidirectional fiber access link. This novel network configuration is based on Infinera's new innovation in Nyquist subcarriers, XR optics, in which a single high-capacity transceiver can be programmed to generate numerous lower-speed subcarriers that can be independently steered to different destinations [7]. In the bidirectional coherent access experiment of Fig. 3(a), the hub can generate/detect 16 independent Nyquist subcarriers, each transmitting/receiving dual polarization 16QAM with a 25Gbps datarate, that can be arbitrarily assigned to up- or downlink communication to/from any of the remote leaf nodes. Each leaf is simply comprised of a single lower-complexity coherent transceiver and a circulator. If optical power is not an issue, the circulator at the leaf can be replaced by a 3dB optical coupler between Tx and Rx to reduce the total cost of the leaf station.

In this example, we assume leaf 1 requests 50Gbps upload and 100Gbps download speed, while leaf 2 requires 50Gbps upload and only 75Gbps download speed. These requests are made to the network provider, which consequently assigns to leaf 1 SCs 3,4 in uplink and SCs 5,6,7,8 in downlink; and leaf 2 is allotted SCs 13,14 in uplink and SCs 10,11,12 in the downlink direction. Also, due to the lower analog front-end bandwidth of leaf 1 and 2, their optical carrier is to be detuned from that of the hub laser and placed approximately in the center of their allocated subcarriers. Figure 3(b) shows an overlay of the described subcarrier-multiplexed channel plan, as well as the location of each node's local oscillator. Note that the other unused SCs (1,2,9,15,16) are reserved for potential bandwidth demand to/from either leaf, as well as being assigned to communicate with other end users.

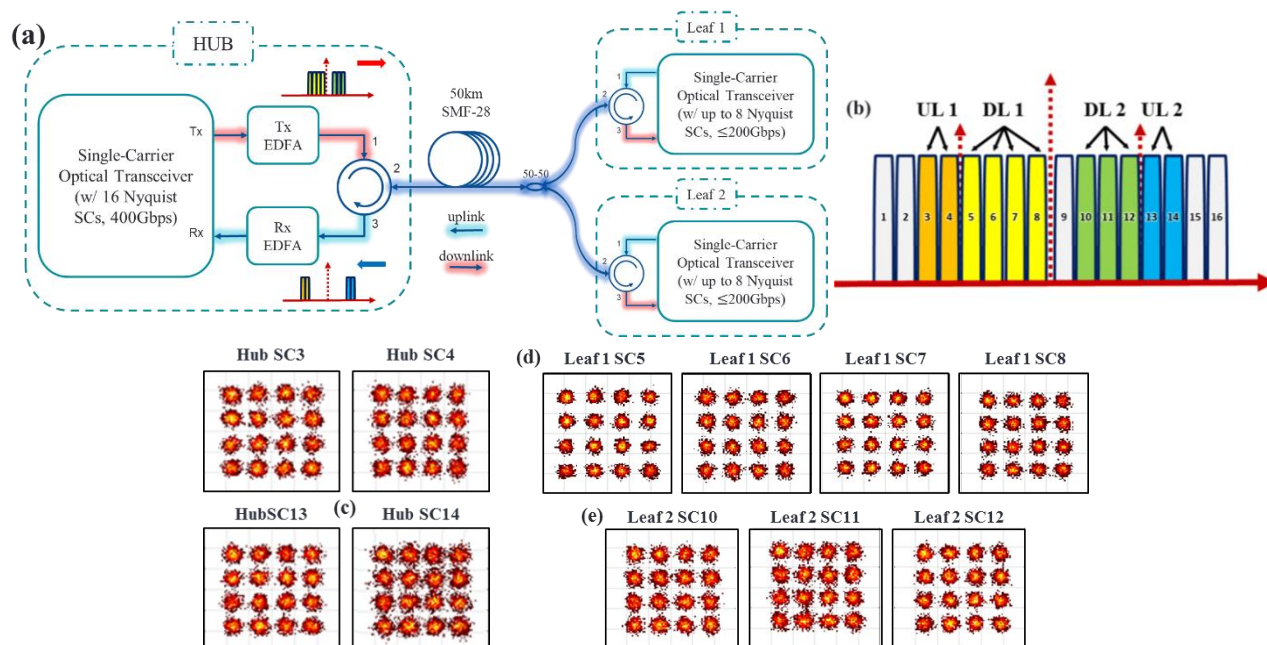


Fig. 3. High-capacity bidirectional coherent access experiments: (a) Experimental setup; (b) Overlay of demonstrated channel plan; Combined constellation diagrams for X and Y polarization at (c) hub receiver (uplink), (d) leaf 1 receiver, (e) leaf 2 receiver

The hub receives uplink data over only 4 SCs: 3, 4 from leaf 1, and 13, 14 from leaf 2. In the other direction, both leaf receivers can see 7 subcarriers being broadcast from the hub (SCs 5,6,7,8,10,11,12), but due to the positioning of their local oscillator and narrower analog front-end bandwidth, only detect the content of their respective assigned SCs (5,6,7,8 for leaf 1 and 10,11,12 for leaf 2). Although not implemented in this experiment, one could envision applying higher layer data encoding per subcarrier that only the hub and each assigned leaf would know. This way data intended for each leaf cannot be detected by other users in the broadcast network. Figures 3(c)-(e) plot the measured constellation diagrams (combined X and Y polarization) at each node of the bidirectional coherent communication setup of Fig. 3(a). It is clear from these plots that error-free bidirectional transmission is successfully accomplished in our novel point-to-multipoint experimental setup, accomplished through Nyquist subcarrier multiplexing between remote end users as well as up- and downlink directions.

4. Conclusion

Utilizing coherent Nyquist subcarrier multiplexing, we successfully demonstrate real-time 2.4Tbps bidirectional coherent DWDM-PON (1.2Tbps in either direction) over a single 100km SMF fiber link. The advantage of the demonstrated method in providing immunity to network reflections and back-scattering are confirmed through measurements. We also propose and experimentally verify a novel high-speed point-to-multipoint bidirectional broadcast network configuration, where a high-capacity aggregation hub communicates with lower-speed remote leaf nodes over different independently controllable coherent optical subcarriers. This proposed network structure breaks the inherent limitations of traditional point-to-point optical access solutions and can pave the way for advances required for 5G, fiber deep, and hyperscale cloud connectivity.

- [1] A. Shahpari, et al., "Coherent Access: A Review," *J. Lightwave Technol.* **35**, 1050-1058 (2017)
- [2] Workshop on "DSP for next generation optical access," ECOC'18, WS08, Rome, Italy (2018).
- [3] H. Rohde, et al., "Coherent Ultra Dense WDM Technology for Next Generation Optical Metro and Access Networks," *J. Lightwave Technol.* **32**, 2041-2052 (2014).
- [4] D. Lavery, et al., "Opportunities for Optical Access Network Transceivers Beyond OOK," *J. Opt. Commun. Netw.* **11**, A186-A195 (2019)
- [5] V. Lal, et al., "Extended C-Band Tunable Multi-Channel InP-Based Coherent Transmitter PICs," *J. Lightwave Technol.* **35**, 1320-1327 (2017).
- [6] D. Krause, et al., "Design Considerations for a Digital Subcarrier Coherent Optical Modem," in *Optical Fiber Comm. Conf.*, (2017).
- [7] Infinera Corporation, "XR Optics: Game-Changing Innovation for Next-Generation Networks," <https://www.infinera.com/innovation/xr-optics>.